Hypercrosslinked polyanilines with nanoporous structure and high surface area: potential adsorbents for hydrogen storage†‡

Jonathan Germain,[a] Jean M. J. Fréchet[ab] and Frantisek Svec*[b]

Received 31st July 2007, Accepted 12th October 2007
First published as an Advance Article on the web 18th October 2007
DOI: 10.1039/b711509a

A method for the preparation of an entirely new type of nanoporous material, hypercrosslinked polyaniline, with permanent porous structure and specific surface areas exceeding 630 $m^2\ g^{-1}$ has been developed. The hypercrosslinking reaction was carried out with commercial polyaniline and diiodoalkanes or paraformaldehyde using both conventional and microwave assisted processes. Polyaniline swollen in an organic solvent was hypercrosslinked to form a rigid, mesh-like structure with permanent porosity and a high surface area. The resulting materials were characterized using infrared spectroscopy and elemental analysis. Porous properties were determined by means of scanning electron microscopy as well as nitrogen and hydrogen adsorption. Short crosslinks such as those formed using paraformaldehyde and diiodomethane led to materials with the highest surface areas. Surface area also increased with the concentration of polyaniline in solution used during preparation. The hydrogen storage capacities of these materials were also tested and a capacity of 2.2 wt% at 77 K and 3.0 MPa was found for the best adsorbent. Hypercrosslinked polyanilines exhibit a remarkably high affinity for hydrogen, which results in enthalpies of adsorption as high as 9.3 kJ mol^{-1} (exothermic), in sharp contrast with hypercrosslinked polystyrenes and metal–organic frameworks for which significantly lower enthalpies of adsorption, typically in the range of 4–7 kJ mol^{-1}, are measured.

Introduction

Nanoporous materials are high surface area solids containing pores with sizes between 1 and 100 nm.[1,2] They have a wide range of applications in areas such as adsorption and separation processes, catalysis, sensors, biotechnology, and microelectronics. The most common representatives of nanoporous materials are carbon, glass, silicates (zeolites), aluminosilicates, oxides, metals, and polymers. Two methods are available for the preparation of the last family of nanoporous materials: (i) direct copolymerization of mixtures containing high percentages of crosslinking monomers and porogenic solvents,[3–7] and (ii) hypercrosslinking.[8–11] Hypercrosslinking involves the dissolution/swelling of a non-crosslinked or slightly crosslinked polymer followed by ''immobilization'' of the pores in their solvated state through a secondary crosslinking process, thus forming pores that persist even after the solvent is removed.

The process most often used for the preparation of hypercrosslinked polymers is shown in Fig. 1. Typically, it has involved polymers based on styrenic precursors. For example, lightly crosslinked poly(divinylbenzene-*co*-vinylbenzyl chloride) beads are prepared using a typical suspension polymerization, then swollen in dichloroethane, acting as solvent, and finally crosslinked using a $FeCl_3$ catalyzed Friedel–Crafts alkylation process. Once the solvent has been removed, the specific surface areas of these polymers can reach well over 2000 $m^2\ g^{-1}$.[11–13] In addition to polystyrene, this methodology has also been used for the preparation of rigid porous polysulfone and polyacrylate networks.[9]

We are now reporting the preparation of novel nanoporous polyaniline. Porous polyaniline has been suggested for use in sensors,[14–16] electrodes,[17,18] and supercapacitors,[18–20] where a porous structure might enhance conductivity and other electronic properties of the polymer. The use of polyaniline as a material for hydrogen storage has also been suggested, although the promising levels of hydrogen adsorption on non-porous polyaniline and polypyrrole that have been claimed[21] could not be reproduced.[22]

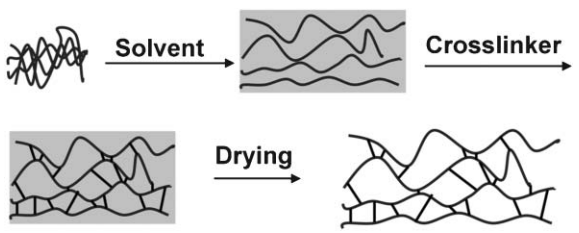

Fig. 1 Schematic representation of the hypercrosslinking process. First, distance is created between polymer chains *via* swelling or dissolution in a solvent. Second, the polymer is crosslinked in its swollen state. Finally, the solvent is removed while rigid crosslinks keep the polymer chains separated, resulting in a material with permanent porosity.

[a]*College of Chemistry, University of California, Berkeley, CA, 94720-1460, USA*
[b]*The Molecular Foundry, Lawrence Berkeley National Laboratory, Berkeley, CA, 94720-8139, USA*
† The HTML version of this article has been enhanced with colour images.
‡ Electronic supplementary information (ESI) available: Water calibration curve for reactor; FTIR spectra for polymers 4 and 12. See DOI: 10.1039/b711509a

Table 1 Specific surface areas reported for porous polyanilines with various morphologies[b]

Morphology	Surface area/m^2 g^{-1} [a]	Reference
Microspheres	80	24
Microspheres	46	23
Nanofibers	55	53
This work (mesh)	632	—

[a] Calculated from nitrogen adsorption using the BET equation. [b] While materials with higher surface areas have been presented,[51,52] these are invariably the result of adding a small amount of polyaniline to a preformed porous material. Since the majority of the resulting material is not polyaniline, we do not consider materials of this type here.

Given the potential of polyaniline in a variety of applications, a significant amount of attention has been directed toward the development of a porous polyaniline structure. The synthetic methods described so far have included the grafting of polyaniline on porous materials, and the use of interfacial polymerization, which produces nanofibers or porous microspheres. For example, porous polyanilines can be prepared using a surfactant-free emulsion process[23] or *via* a bubble-induced mechanism[24] that leads to pores ranging in size from 10 to 300 nm. Another approach has involved the deposition of polyaniline onto high surface area carbon.[19] Table 1 shows that the specific surface areas of porous polyanilines reported thus far are modest, typically up to 80 m^2 g^{-1}. While these surface areas far exceed that of a non-porous polymer, they do not approach the values that have been achieved for polystyrene-based porous polymers.[11,12,25] We now report the preparation of nanoporous polyaniline using the hypercrosslinking approach. To achieve this, we identified reactions that enable the post-crosslinking of a linear polyaniline base and developed conditions leading to the formation of materials with high surface areas.

Results and discussion

Preparation of hypercrosslinked polyaniline

The hypercrosslinking process includes swelling/dissolution of the polymer in a solvent followed by addition of a bifunctional reagent that crosslinks the solvated chains and preserves their spatial distribution even after the solvent is removed, leaving behind a network of intercommunicating pores. Depending on its state (reduced: leucoemeraldine; 50% oxidized: emeraldine), polyaniline contains a number of amine and/or imine functionalities that can be alkylated.[26] Typically, N-alkylation is achieved using alkyl halides. Since we target crosslinking, bifunctional alkylating agents must be used and to compensate for the limited reactivity of polyaniline, the more reactive α,ω-diiodoalkanes were chosen over dichloro- and dibromoalkanes. The reaction path we used is shown in Scheme 1A. The alkylation reactions generally proceeded rather slowly when performed under standard reaction conditions. Significantly faster reaction kinetics were obtained using a microwave-assisted process that enables the use of higher reaction temperatures and sealed vials to prevent evaporation of volatile reagents and solvents. Although Scheme 1A only shows the crosslinking of emeraldine base polyaniline, both

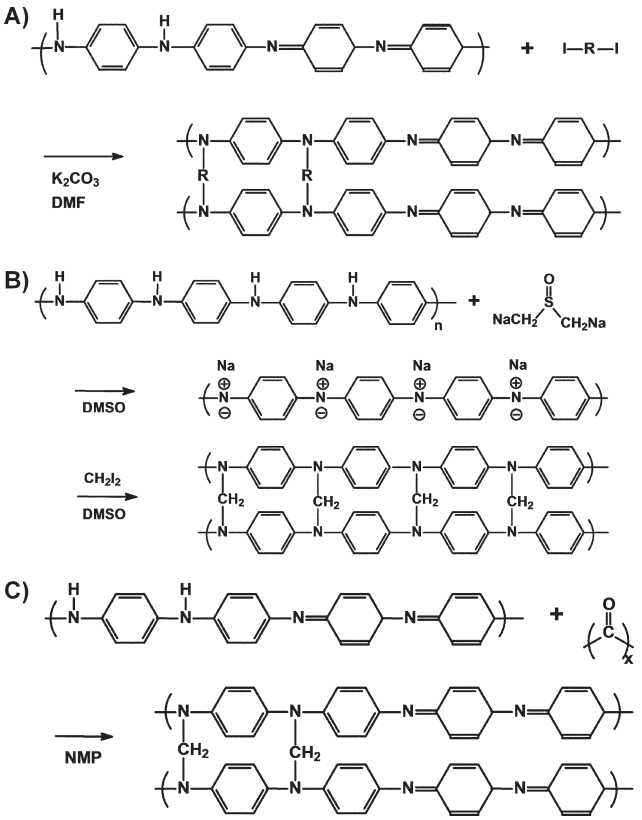

Scheme 1 Simplified reaction schemes showing the preparation of hypercrosslinked polyaniline using single step crosslinking with diiodoalkanes (A), dimethylsulfoxide-assisted two-step crosslinking with diiodomethane (B) and crosslinking with paraformaldehyde (C).

emeraldine and leucoemeraldine bases were used in these experiments as shown in Tables 2 and 3. In addition, diiodoalkanes of differing lengths were tested to investigate the effect of crosslink length on surface area and porous properties. Fig. 2 compares the specific surface areas of porous polyanilines prepared under comparable conditions using three different crosslinkers. SEM images of the porous polymer 4 in the protonated form shown in Fig. 3 reveal a mesh-like nanostructure that is homogeneous in appearance and similar in morphology to hypercrosslinked polystyrene.[12] Although some larger pores are clearly visible, the nanopores that account for most of the surface area in the polymer are smaller than the resolution of the microscope.

FTIR spectra of the hypercrosslinked polyanilines clearly demonstrate the presence of an alkylated polyaniline base. For example, the spectrum of polymer 4, which was crosslinked with diiodomethane, exhibits a C–N stretching band at ~1295 cm^{-1}. A small N=Q=N quinoid stretching band is also visible at 1108 cm^{-1}.[24] While the precursor for polymer 4 was leucoemeraldine polyaniline, it is possible that quinoid regions reappeared because segments of non-crosslinked polyaniline had the opportunity to oxidize in air during the Soxhlet extraction step. Bands near 1500 and 1600 cm^{-1}, characteristic of the stretching of benzenoid and quinoid rings, are slightly upshifted. This observation is in good agreement with literature data concerning the N-alkylation of polyaniline.[27]

Table 2 Porous properties of leucoemeraldine polyaniline hypercrosslinked with diiodoalkanes in DMF using the microwave-assisted process

Entry	Crosslinker	$C_{polyaniline}$/g mL^{-1}	Surface area/m^2 g^{-1}		$V_{p,tot}$[c]/cm^3 g^{-1}	$V_{p,nano}$[d]/cm^3 g^{-1}	H_2[e] (wt%)	ΔH_{ads}[f]/kJ mol^{-1}
			BET[a]	Langmuir[b]				
1	Diiodomethane	0.019	120	186	0.43	0.05	0.46	5.0
2	Diiodomethane	0.028	222	360	0.89	0.10	0.18	8.8
3	Diiodomethane	0.034	332	322	0.78	0.16	0.24	7.9
4	Diiodomethane	0.038	439	326	0.78	0.20	0.51	7.8
5	Diiodomethane	0.058	493	327	0.78	0.23	0.73	7.4
6	Diiodomethane	0.076	632	396	0.94	0.29	0.96	7.5
7	Diiodoethane	0.039	47	128	0.32	0.02	0.11	5.7
8	Diiodopropane	0.039	20	30	0.08	0.01	0.06	—

[a] Calculated from nitrogen adsorption isotherms using the BET equation. [b] Calculated from hydrogen adsorption isotherms using the Langmuir equation. [c] Total pore volume calculated from nitrogen adsorption at a relative pressure of 0.99. [d] Nanopore volume estimated from nitrogen adsorption at a relative pressure of 0.25. [e] Hydrogen storage capacity at 77 K and 0.12 MPa. [f] Peak enthalpy of adsorption of hydrogen calculated using the van't Hoff equation based on adsorption isotherms measured at 77 and 87 K.

Table 3 Porous properties of polyanilines hypercrosslinked using conventional processes

Entry	Polyaniline type	Synthesis	Surface area/m^2 g^{-1}		H_2[c] (wt%)	$V_{p,tot}$[d]/cm^3 g^{-1}	$V_{p,nano}$[e]/cm^3 g^{-1}
			BET[a]	Langmuir[b]			
9	Emeraldine	Diiodomethane	426	323	0.77	0.32	0.20
10	Leucoemeraldine	DMSO-assisted diiodomethane	36	44	0.11	0.11	0.02
11	Emeraldine	Paraformaldehyde	0	0	0	0	0

[a] Calculated from nitrogen adsorption isotherms using the BET equation. [b] Calculated from hydrogen adsorption isotherms using the Langmuir equation. [c] Hydrogen storage capacity at 77 K and 0.12 MPa. [d] Pore volume calculated from nitrogen adsorption at a relative pressure of 0.99. [e] Nanopore volume estimated from nitrogen adsorption at a relative pressure of 0.25.

It is conceivable that the reaction with diiodomethane also affords some quaternized nitrogen functionalities. If such a quaternization reaction occurred despite the severe steric constraints that exist, these quaternized amines would be accompanied by iodide counterions. However, elemental analysis of polymers 1, 4, and 7 did not reveal the presence of any detectable amounts of iodine suggesting that quaternization did not take place to any significant extent. This is confirmed by FT-IR analysis of the polymer showing no split peaks as would be expected if some quaternization had taken place, and strong peaks at 3380–3390 cm^{-1} characteristic of polyaniline base for both polymers 4 and 12.[28]

Since the solubility of polyaniline is limited even in solvents such as NMP and DMF, we also carried out crosslinking of the sodium salt of polyaniline, which is more soluble than the base.[27] Deprotonation of polyaniline was achieved using the sodium salt of DMSO as shown in Scheme 1B. The resulting polyaniline salt, which is highly soluble in DMSO, was then crosslinked using diiodomethane; the result obtained is shown in Table 3. Clearly, this two-step procedure does not afford a material with the desired high surface area. Crosslinking the sodium salt of polyaniline in DMSO only affords products with specific surface areas of less than 50 m^2 g^{-1}. While the polyaniline salt dissolves well in DMSO, polyaniline base itself is less soluble in this solvent. Given its lack of ionic character, the crosslinked product likely begins to de-solvate early in the crosslinking process, before enough crosslinks are formed to afford a rigid structure. The crosslinking of polyaniline then continues in a less

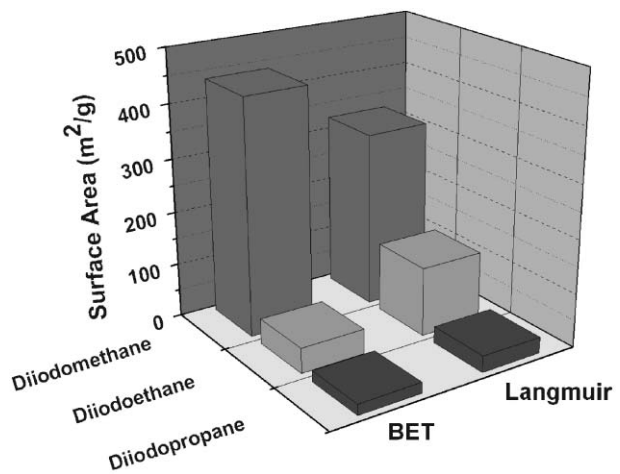

Fig. 2 Specific surface areas of nanoporous polyanilines hypercrosslinked with diiodomethane, diiodoethane and diiodopropane using a polyaniline concentration of 0.04 g mL^{-1}. Surface areas were calculated from nitrogen adsorption isotherms using the BET equation and hydrogen adsorption isotherms using the Langmuir equation.

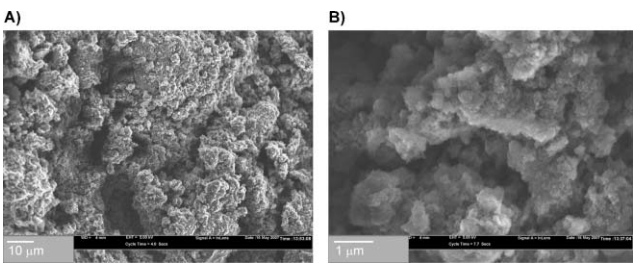

Fig. 3 SEM micrographs of hypercrosslinked leucoemeraldine polyaniline 4 after protonation with HCl at magnifications of 1000× (A) and 15000× (B).

Table 4 Porous properties of polyaniline hypercrosslinked with paraformaldehyde using the microwave-assisted process

Entry	Polyaniline type	FA[a]	Surface area/m^2 g^{-1}		$V_{p,tot}$[d]/cm^3 g^{-1}	$V_{p,nano}$[e]/cm^3 g^{-1}	H_2[f] (wt%)	ΔH_{ads}[g]/kJ mol^{-1}
			BET[b]	Langmuir[c]				
12	Emeraldine	2.4	480	351	0.55	0.21	0.82	9.3
13	Leucoemeraldine	3.7	141	184	0.41	0.06	0.44	7.0
14	Leucoemeraldine	2.4	175	267	0.65	0.08	0.60	6.7
15	Leucoemeraldine	4.8	141	186	0.54	0.07	0.44	7.2

[a] Equivalents of paraformaldehyde relative to the amine content of polyaniline. [b] Calculated from nitrogen adsorption isotherms using the BET equation. [c] Calculated from hydrogen adsorption isotherms using the Langmuir equation. [d] Pore volume calculated from nitrogen adsorption at a relative pressure of 0.99. [e] Nanopore volume estimated from nitrogen adsorption at a relative pressure of 0.25. [f] Hydrogen storage capacity at 77 K and 0.12 MPa. [g] Peak enthalpy of adsorption of hydrogen calculated using the van't Hoff equation based on adsorption isotherms measured at 77 and 87 K.

solvated state and leads to a product with significantly smaller surface area and pore volume.

Paraformaldehyde is another reagent that can be used to hypercrosslink polyaniline without risk of quaternization.[29] Scheme 1C shows the reaction scheme used to crosslink polyaniline with paraformaldehyde. The conventional method we tested first led to a solid insoluble product with no appreciable surface area (Table 3). The volatility of gaseous formaldehyde appears to be one of the reasons for the failure of this early attempt. Further attempts using the microwave-assisted approach within sealed vials were much more successful affording the solid, hypercrosslinked products with high surface areas listed in Table 4. The features of the FTIR spectrum of polymer 12, used as an example for hypercrosslinked polymers produced by this approach, are only slightly different from those observed in the spectrum of polymer 4. In particular, polymer 12 has a broadened C–N stretching peak.

Porous properties

Nitrogen adsorption isotherms measured at 77 K were used to characterize the porous structures of the hypercrosslinked polymers. The type 4[30] isotherms observed for polymers prepared using the single step crosslinking with diiodomethane and paraformaldehyde indicate the presence of both nanopores, which fill with nitrogen at low pressure, and macropores, which fill with nitrogen as the pressure increases. The limited adsorption of nitrogen onto polymers hypercrosslinked using 1,2-diiodoethane and 1,3-diiodopropane as well as the DMSO-assisted method suggests a lack of substantial pore structure. In hypercrosslinking, the purpose of the crosslinks is to prevent pores from collapsing during solvent removal. The trend described above, and in particular the precipitous drop in surface area caused by the change from diiodoethane to diiodopropane, suggests that the rigidity of the crosslinks is critical to the formation of a high surface area material.

Table 2 details the effect of polyaniline concentration in the reaction mixture on the surface area of leucoemeraldine polyaniline crosslinked with diiodomethane. The BET surface area increases monotonically as the concentration of polyaniline increases. The Langmuir surface area increases as well, though this increase is not monotonic. The generally accepted mechanism of hypercrosslinking suggests that pore formation is related to the interplay between the rate of crosslinking and the rate of solvent rejection from the partially crosslinked polymer. We speculate that higher reaction rates achieved at higher concentrations increase the number of pores created in a fully solvated state. This then leads to formation of more pores that are accessible to nitrogen. Since part of this pore formation occurs at the expense of pores that are accessible only to hydrogen, these effects result in the differing slopes of the BET and Langmuir surface area curves.

It should also be noted that the ratio of surface area, as calculated using the BET equation, to nanopore volume is nearly constant at around 2200 m^2 mL^{-1} for all samples of leucoemeraldine base crosslinked with diiodomethane. Although this analysis and the nanopore volume calculation itself consider only pores that are large enough to be detected using nitrogen adsorption, this provides some insight into these materials. Since the relationship between apparent surface area and pore volume is a function of the nanopore size distribution, this suggests that the nanopore size distributions for these materials are very similar.

Fig. 4 illustrates the effect of the method used for hypercrosslinking on the specific surface area of the resulting nanoporous polymer. While the single step approaches afford products with surface areas in hundreds of m^2 g^{-1}, products prepared using the two-step DMSO-assisted process have

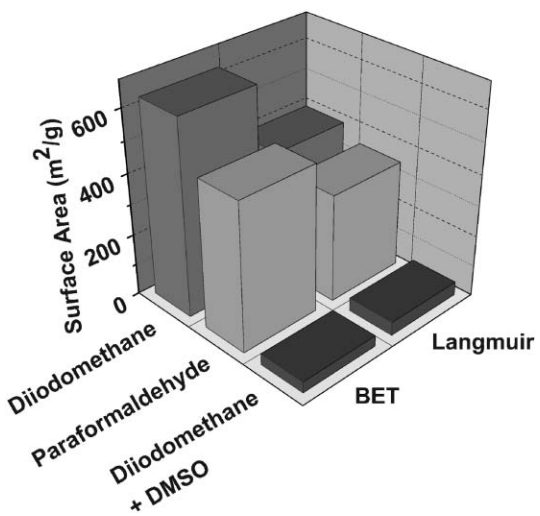

Fig. 4 Specific surface areas of nanoporous polyanilines hypercrosslinked using diiodomethane, paraformaldehyde, and diiodomethane assisted with dimethylsulfoxide. Data calculated from nitrogen adsorption using the BET equation and hydrogen adsorption using the Langmuir equation.

substantially smaller surface areas. The crosslinking of polyaniline base with diiodomethane and paraformaldehyde leads to polymers with the largest specific surface areas, reaching values of 630 and 390 $m^2\ g^{-1}$ as calculated from nitrogen adsorption isotherms using the Brunauer–Emmett–Teller (BET) and Langmuir equations, respectively. This difference in surface areas is typical for data obtained using these two methods. While the BET method, which uses adsorption of a gas such as nitrogen in a subcritical state, is the most common method of determining the surface area of porous materials, it is known to afford inflated values for materials that contain nanopores.[31] The Langmuir equation is used in conjunction with hydrogen adsorption isotherms measured in a supercritical state and provides an alternative to BET. The surface areas of most of polymers prepared in this work far exceed those shown in Table 1 for polyaniline microspheres or microfibers, but remain well below the 2000 $m^2\ g^{-1}$ obtained with hypercrosslinked polystyrene.[11,12] This difference may be attributed to the dissimilar character of the crosslinking reactions. A completely hypercrosslinked polystyrene features two crosslinks per aromatic ring while fully reacted, non-quaternized, hypercrosslinked polyaniline has only one. In addition, the selection of the type of thermodynamically compatible solvents that are required for good hypercrosslinking is much richer for poly(chloromethylstyrene) than for polyaniline.

Hydrogen storage

Nanoporous polymers have recently emerged as promising materials for hydrogen storage.[12,13,25] Early reports have claimed[21] or predicted[32] high levels of hydrogen adsorption in polyaniline. The low-pressure testing of the hydrogen storage capacity of our nanoporous polyanilines is summarized in Tables 2–4. Some of the more promising polymers were also tested for hydrogen adsorption at higher pressures. As shown in Fig. 5, polymer 6 has an adsorption capacity of 2.2 wt% at 77 K and 3.0 MPa.

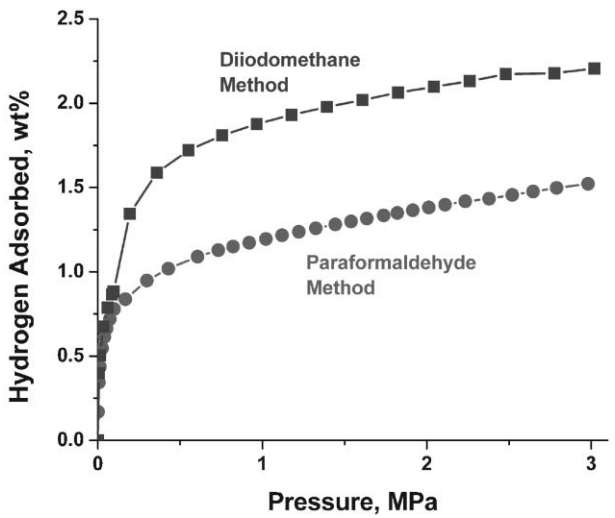

Fig. 5 Hydrogen adsorption isotherms determined for polyaniline 12 hypercrosslinked with paraformaldehyde (circles) and 6 hypercrosslinked with diiodomethane (squares).

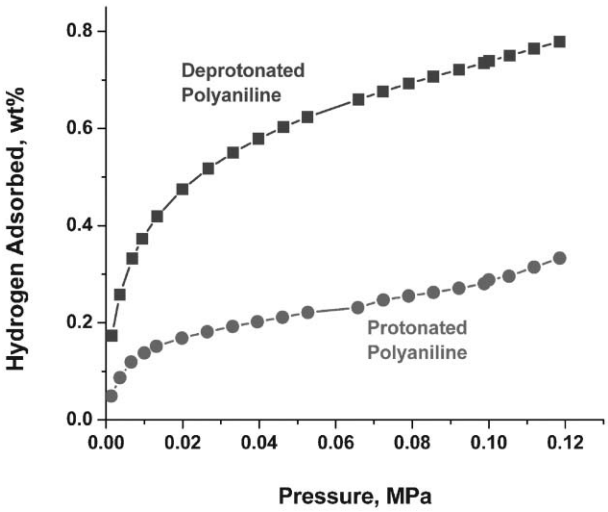

Fig. 6 Hydrogen adsorption isotherms measured using leucoemeraldine polyaniline 4 hypercrosslinked using diiodomethane before (squares) and after (circles) protonation with HCl at pressures of 0 and 0.12 MPa.

Protonation of hypercrosslinked polyaniline severely decreases its ability to physisorb hydrogen at 77 K. As shown in Fig. 6, the hydrogen adsorption capacity of polymer 4 at 0.12 MPa is 0.8 wt% before protonation but drops to only 0.3 wt% after its treatment with HCl. Aromatic rings are an important adsorption site for hydrogen in materials of this type.[33–35] It has also been suggested that aromatic rings that contain electron donating groups adsorb hydrogen more easily than those bearing electron withdrawing functionalities.[36] While the aniline functionality is strongly electron donating, the quaternary ammonium group formed upon protonation of polyaniline is electron withdrawing and thus decreases the ability of the polymers to adsorb hydrogen. No significant room temperature hydrogen adsorption onto polymer 4 was noted after protonation.

An ideal nanoporous material for hydrogen storage should possess a high adsorption capacity to accommodate as much hydrogen as possible and, simultaneously, its enthalpy of adsorption should be sufficiently high to achieve the desired adsorption at ambient temperature. Most of the currently known porous materials including polymers, metal–organic frameworks, and carbon have rather low enthalpies of adsorption and show a rapid decrease in activity as the most active sites become saturated.[12,25,32,37,38] This is also why the vast majority of hydrogen adsorption studies are run at 77 K. Fig. 7 compares the apparent enthalpies of adsorption of hydrogen in polyanilines 4 and 12 hypercrosslinked with diiodomethane and formaldehyde, respectively, and a hypercrosslinked polystyrene we have studied previously.[12] The enthalpy of adsorption measured for emeraldine base polyaniline hypercrosslinked with paraformaldehyde reaches a value of 9.3 kJ mol^{-1} (exothermic), significantly higher than those found for either leucoemeraldine base polyaniline hypercrosslinked with diiodomethane or hypercrosslinked polystyrene. Interestingly, while for most porous hydrogen storage materials the affinity for hydrogen rapidly decreases as their surface is covered, the opposite trend is observed for

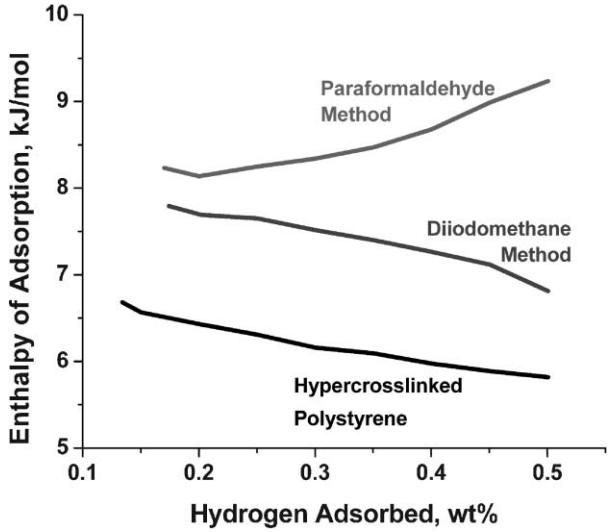

Fig. 7 Enthalpy of exothermic adsorption of hydrogen onto polyaniline hypercrosslinked with diiodomethane (polymer 4) and paraformaldehyde (polymer 12), compared with the enthalpy of adsorption onto hypercrosslinked polystyrene.

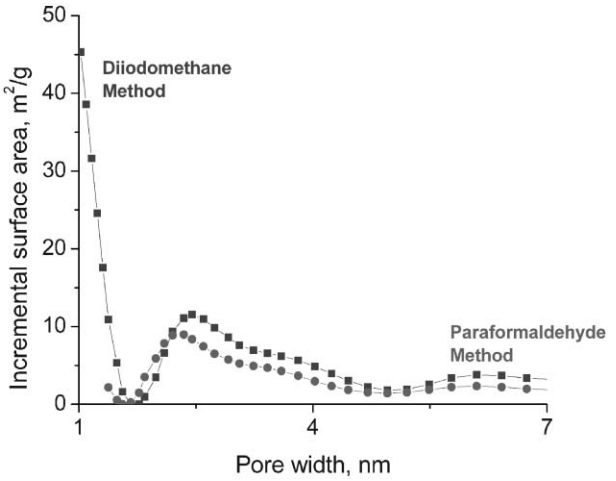

Fig. 8 Incremental surface areas for hypercrosslinked polyanilines 12 (circles) and 6 (squares) prepared using paraformaldehyde and diiodomethane, respectively, as calculated using the Tarazona DFT method.

polyaniline hypercrosslinked with paraformaldehyde. The enthalpy of adsorption determined for this polymer grows over the range of coverage we studied. One possible explanation for this unexpected trend is the presence of net attractive interactions between adsorbed species. Another possibility involves changes in the morphology of the polymer due to swelling during adsorption of gas. It is clear that the slope of this curve must eventually change and that the enthalpy of adsorption will decrease as the surface fills further. Since the increase is observed only for polyaniline hypercrosslinked with paraformaldehyde and not for its counterpart crosslinked with diiodomethane, it is likely that some yet to be determined material property is responsible for this behavior. In contrast, leucoemeraldine base polyanilines hypercrosslinked with formaldehyde under the same conditions have enthalpies of adsorption in the range of 6.7–7.2 kJ mol^{-1} (Table 4). Our experiments do not show any significant effect of the concentration of paraformaldehyde used in the reaction mixture on the enthalpy of adsorption of the resulting material.

While most metal–organic frameworks (MOF) and porous carbons exhibit enthalpies of adsorption from 4–7 kJ mol^{-1},[39] Dinca *et al.* have designed MOFs with exposed magnesium[40] and copper[41] centers, which exhibit enthalpies of adsorption of 9.5 and 10.1 kJ mol^{-1}, respectively. Unlike the materials presented in this work, these systems rely on the presence of coordinatively unsaturated metal centers to enable interactions that lie on the edge between physisorption and chemical reaction. While this is an interesting approach, it produces materials that react irreversibly with ambient air and thus require special handling procedures. In contrast, our sorbents do not need any special care. Oxidation has been used to increase the adsorption enthalpy of some nanostructured carbons affording sorbents with enthalpies of adsorption of 7.5 kJ mol^{-1}.[42]

Polyanilines hypercrosslinked with diiodomethane also exhibit adsorption enthalpies larger than those determined for many other porous materials (Table 2). The highest enthalpy of adsorption found was 8.8 kJ mol^{-1} for polymer 2. There is no clear relationship between enthalpy of adsorption and the concentration of polyaniline in the precursor solution.

Two of the primary theoretical justifications for the high enthalpies of adsorption exhibited by hypercrosslinked polyanilines are (i) enhanced H_2–polymer interactions due to the presence of an electron donating group on the aromatic ring[35] and (ii) the presence of small pores in the polymer. These pores increase adsorption enthalpy by allowing hydrogen to interact with multiple pore walls simultaneously.

Fig. 8 shows the apparent pore size distributions for two of our hypercrosslinked polyanilines. It is worth noting that current methods available for the determination of pore size distribution in materials with small pores do not account for either swelling of the polymer matrix or surface heterogeneity. Since hypercrosslinked polymers swell in even the most thermodynamically unfavorable solvents,[11] they might swell in nitrogen as well. Swelling of the polymer tends to increase their pore size relative to the dry state. Unlike the hypercrosslinked polystyrenes we presented earlier,[12] the swelling of hypercrosslinked polyanilines is not restricted by the state of the precursor. Thus, our pore size distribution plots serve only as a general guide to the properties of the material.

Several studies describe polymers of intrinsic microporosity (PIMs) with substantial presence of very small pores.[43,44] For example, Ghanem *et al.* determined that the distribution of pores in their triptycene-based PIMs is centered around 0.7 nm.[45] McKeown *et al.* synthesized a series of nanoporous PIMs with pores of approximately the same size.[46] Also, hypercrosslinked polystyrenes have been reported with pore sizes that range from 1 to 1.8 nm.[12,13] The pore size distributions shown in Fig. 8 indicates that polymer 6 has more pores with sizes in the 1 nm range than polymer 12. However, these two polymers appear to have similar extents of surface area in pores centered around 3 nm. While limitations in techniques, in particular with regard to the effects of swelling and surface heterogeneity, make direct comparisons

of these results difficult, it is reasonable to suggest that both the hypercrosslinked polyanilines and the PIMs have substantial surface areas in pores smaller than 1 nm.

Experimental

Materials and equipment

Polyaniline (MW 5000, batch 07106JE), diiodomethane, 1,2-diiodoethane and 1,3-diiodopropane were purchased from Aldrich (St. Louis, MO). Paraformaldehyde was purchased from Fisher. Dimethylformamide was purified using a solvent purification system[47] before use. All other solvents were of the best available quality and used without additional purification.

Hydrogen (99.999% purity) and nitrogen (99.9995% purity) adsorption measurements at pressures of up to 0.12 MPa were carried out on a Micromeritics ASAP 2020 (Norcross, GA) surface area and porosity analyzer as described previously.[12] The porous polymers were degassed at 110–115 °C. High pressure hydrogen adsorption measurements were carried out with a PCT Pro 2000 (Hy-Energy, Newark, CA). Samples were first degassed on the ASAP 2020 instrument, then moved to a nitrogen filled glove box where they were transferred into the PCT Pro 2000 sample holder. Measurements using pressures of up to 3.0 MPa were carried out in a microdoser with the sample holder placed in a Dewar containing liquid nitrogen or liquid argon.

Microwave-assisted reactions were conducted in a Biotage Initiator 2.0 (Biotage, Inc., Uppsala, Sweden). Since different microwave reactors even of the same model can produce different results, the water calibration curve for the reactor used in this work is presented in the ESI.‡

SEM images were taken using a FESEM Ultra 55 (Carl Zeiss, Inc.). Polyaniline was protonated with HCl before imaging.

Elemental analyses were conducted by Quantitative Technologies, Inc. (Whitehouse, NJ).

Infrared spectra were collected using an Excalibur 3100 FT-IR (Varian, Inc., Palo Alto, CA). Thoroughly dry samples were mixed with KBr and formed into pellets within a nitrogen filled glove box. The resulting KBr pellets were transported to the IR spectrometer and characterized as quickly as possible. FTIR spectra are available in the ESI.‡

The Brunauer–Emmett–Teller (BET) equation was used to calculate specific surface areas based on nitrogen adsorption isotherms measured at 77 K and relative pressures approaching 1.0. The Langmuir equation was used to calculate specific surface areas based on hydrogen adsorption isotherms measured at 77 K and pressures of up to 0.12 MPa. Calculations using density functional theory (DFT) were carried out using the Tarazona DFT[48,49] portion of the DFT Plus software (Micromeritics) with the regularization set to 0.1000.

Preparation of leucoemeraldine polyaniline

Leucoemeraldine polyaniline was synthesized using a modified method of Moon *et al.*[50] In a typical synthesis, 100 mL of water was added to 10.4 g of emeraldine base polyaniline and 21.4 g of sodium dithionite. Another 10.3 g portion of dithionite was added after 6 h. The dispersion was allowed to stir overnight, and the solid then decanted in 1.5 L of water that had first been purged with nitrogen to lower its oxygen content. After separation, the solid polymer was dried *in vacuo* at room temperature and stored in a desiccator under vacuum. The reduction to leucoemeraldine polyaniline was verified by the disappearance of the peak at about 630 nm in the UV-vis spectrum.[50]

Preparation of hypercrosslinked polyanilines

Conventional method of hypercrosslinking of emeraldine base polyaniline with diiodomethane. In a typical synthesis, 1.10 g of emeraldine base polyaniline and 7.38 g of potassium carbonate were placed in a flask and 40 mL of DMF added followed by addition of 6.2 g of diiodomethane. The mixture was then reacted under dry nitrogen and reflux for 3 days with a condenser cooled to below 0 °C.

Microwave-assisted hypercrosslinking of emeraldine base polyaniline with diiodomethane. In a typical synthesis, 0.17 g of emeraldine base polyaniline and 1.10 g of potassium carbonate were placed in a dry microwave vial and 5 mL of DMF added. The vial was flushed with dry nitrogen and the polyaniline allowed to dissolve. Then 1.03 g of diiodomethane was added, the vial sealed and placed in a microwave reactor. The reaction was carried out at 200 °C for 8 minutes.

Microwave-assisted hypercrosslinking of leucoemeraldine base polyaniline with diiodoalkanes. Leucoemeraldine base polyaniline and 3.8 equivalents of potassium carbonate were placed in a dry microwave vial under dry nitrogen flow and DMF added to achieve the concentration of polyaniline shown in Table 2. A typical synthesis used 3–5 mL of solvent. The polymer was allowed to dissolve for a few minutes. Using a syringe, 4 equivalents (relative to amino groups in polyaniline) of the appropriate diiodoalkane were added and the vial sealed. The vial was then placed in the microwave reactor, stirred for 4 minutes at room temperature and allowed to react first at 110 °C for 4 minutes and then at 170 °C for another 10 minutes.

Dimethylsulfoxide-assisted hypercrosslinking of leucoemeraldine base polyaniline with diiodomethane. In a typical synthesis, 0.98 g of sodium hydride was placed in a dry flask under dry nitrogen and 10 mL of dry DMSO was added. The mixture was allowed to react for 24 h before an additional 60 mL of DMSO was added. Then, 1.47 g of leucoemeraldine polyaniline was admixed and allowed to stir at 60 °C for 36 h. Finally, 2.0 mL of diiodomethane was added to the mixture and the reaction allowed to continue for 2 days. The polymer was then separated and rinsed with alternating aliquots of DMF and water.

Conventional method of hypercrosslinking of emeraldine base polyaniline with paraformaldehyde. Paraformaldehyde was used to hypercrosslink polyaniline using a modified procedure described by Giumanini *et al.*[29] Specifically, 1.64 g of emeraldine base polyaniline was added to a flask containing 50 mL of dry DMF held under dry nitrogen followed by

addition of 0.31 g of paraformaldehyde and the flask heated under a reflux condenser to 120 °C overnight. Then 0.30 g paraformaldehyde was added to the mixture After 4 h another 0.28 g paraformaldehyde was added and the reaction was then allowed to continue overnight.

Microwave-assisted hypercrosslinking of polyaniline with paraformaldehyde. In a typical synthesis, 0.35 g polyaniline was placed in a dry microwave vial under dry nitrogen and 5 mL of anhydrous *N*-methyl pyrrolidinone (NMP) added. The polyaniline was allowed to dissolve for a few minutes, then paraformaldehyde was quickly added and the vial sealed. The exact quantities of paraformaldehyde used are shown in Table 4. Alternatively, polyaniline and paraformaldehyde were mixed together and placed in a microwave vial before addition of NMP. The vial was placed in a microwave reactor and the reaction carried out at 120 °C for 2 h, followed by 250 °C for 4 h.

Recovery and purification of hypercrosslinked polyanilines. Following each hypercrosslinking reaction, the polymer was recovered and extracted with DMF in a Soxhlet apparatus until the solvent around the thimble was visually clear for at least one day. The polymers were recovered by filtration and then placed in a saturated solution of NaOH in methanol for a few minutes. Finally, the solid was rinsed with water until the effluent had a neutral pH. To speed drying, the polymers were then rinsed with diethyl ether before being dried *in vacuo* at room temperature. To minimize physisorption of water and carbon dioxide, all hypercrosslinked polyanilines were handled quickly when in air and stored either in a glove box under N_2 or in a desiccator under vacuum.

Protonation of polyaniline. Hypercrosslinked leucoemeraldine polyaniline 4 (Table 2) was rinsed with a solution of 1 mol L^{-1} HCl in water, then rinsed with water until the effluent had a pH of 7. The polymer was then dried *in vacuo via* the degas procedure described earlier. Protonation of hypercrosslinked polyaniline 4 was verified by elemental analysis. No chlorine was detected in polyaniline prior to protonation while after exposure to HCl a Cl : N ratio of 4 : 10 was found.

Conclusions

Nanoporous polyanilines can be prepared using hypercrosslinking of commercially available polyaniline with diiodoalkanes or formaldehyde. Some of these polymers exhibit specific surface areas exceeding 630 $m^2\ g^{-1}$ that are unprecedented for this class of polymers. As shown in Table 1, this value is significantly larger than the 40–80 $m^2\ g^{-1}$ previously reported for porous polyanilines. Materials with the highest surface areas were obtained using either diiodomethane or formaldehyde, reagents that lead to formation of rigid crosslinks. The porous properties are a function of the concentration of polyaniline in the reaction mixture.

Our preliminary experiments indicate that these materials have a certain potential for hydrogen storage. Although their overall hydrogen storage capacity at 77 K is currently lower than that of our hypercrosslinked polystyrene,[12,33] they offer the highest enthalpy of adsorption of any air-stable sorbent-type hydrogen storage material. Further optimization of reaction conditions is expected to lead to materials with much higher surface areas and therefore enhanced hydrogen storage capacities. In addition, porous polyanilines have potential applications in the area of electronic materials, especially those areas that would benefit from the nanoscale mixing of a soluble polymer in the network of an insoluble one.

References

1 *Nanoporous Materials: Science and Engineering*, ed. G. Q. Lu and X. S. Zhao, Imperial College Press, Singapore, 2004.
2 The IUPAC recommendation on nomenclature divides porous materials according to the size of pores to macroporous with pores larger than 50 nm, mesoporous with pore size in the range 2–50 nm, and microporous containing pores smaller than 2 nm. The name for the latter category is confusing since it includes the prefix micro but clearly concerns only nanopores. In order to avoid any misunderstanding, we use only the expression nanopores.
3 J. Seidl, J. Malinsky, K. Dusek and W. Heitz, *Adv. Polym. Sci.*, 1967, **5**, 113–213.
4 A. Revillon, A. Guyot, Q. Yuan and P. dePrato, *React. Polym.*, 1989, **10**, 11–25.
5 D. C. Sherrington, *Macromol. Symp.*, 1993, **70**(71), 303–314.
6 D. C. Sherrington, *Chem. Commun.*, 1998, 2275–2286.
7 O. Okay, *Prog. Polym. Sci.*, 2000, **25**, 711–779.
8 V. A. Davankov, *React. Polym.*, 1990, **13**, 27–42.
9 M. P. Tsyurupa, *React. Funct. Polym.*, 2002, **53**, 193–203.
10 M. P. Tsyurupa and V. A. Davankov, *React. Funct. Polym.*, 2006, **66**, 768–779.
11 J. Ahn, J. Jang, C. Oh, S. Ihm and D. C. Sherrington, *Macromolecules*, 2005, **39**, 627–632.
12 J. Germain, J. Hradil, J. M. J. Fréchet and F. Svec, *Chem. Mater.*, 2006, **18**, 4430–4435.
13 J. Y. Lee, C. D. Wood, D. Bradshaw, M. J. Rosseinsky and A. I. Cooper, *Chem. Commun.*, 2006, 2670–2672.
14 S. Virji and R. B. Kaner, *J. Phys. Chem. B*, 2006, **110**, 22266–22270.
15 G. E. Collins, *Synth. Met.*, 1996, **78**, 93–101.
16 J. Janata, *Nat. Mater.*, 2003, **2**, 19–24.
17 F. Fusalba, P. Gouerec, D. Villers and D. Belanger, *J. Electrochem. Soc.*, 2001, **148**, A1–A6.
18 K. Rossberg, G. Paasch and L. Dunsch, *J. Electroanal. Chem.*, 1998, **443**, 49–62.
19 W. C. Chen, T. C. Wen and H. S. Teng, *Electrochim. Acta*, 2003, **48**, 641–649.
20 S. K. Mondal, K. Barai and N. Munichandraiah, *Electrochim. Acta*, 2007, **52**, 3258–3264.
21 S. J. Cho, S. S. Kwang, T. H. Kim and K. Choo, *Prepr. Pap.–Am. Chem. Soc., Div. Fuel Chem.*, 2002, 47.
22 B. Panella, L. Kossykh, U. Detlaff-Weglikowska, M. Hirscher, G. Zerbi and S. Roth, *Synth. Met.*, 2005, **151**, 208–210.
23 Y. J. He, *Mater. Lett.*, 2005, **59**, 2133–2136.
24 J. M. Du, Z. M. Liu, B. X. Han, Z. H. Li and J. L. Zhang, *Microporous Mesoporous Mater.*, 2005, **84**, 254–260.
25 C. D. Wood, B. Tan, A. Trewin, H. Niu, D. Bradshaw, M. J. Rosseinsky, Y. Z. Khimyak, N. L. Campbell, R. Kirk, E. Stockel and A. I. Cooper, *Chem. Mater.*, 2007, **19**, 2034–2048.
26 B. Z. Zhao, K. G. Neoh and E. T. Kang, *Chem. Mater.*, 2000, **12**, 1800–1806.
27 W. Y. Zheng, K. Levon and J. Laakso, *Macromolecules*, 1994, **27**, 7754–7768.
28 Z. Ping, G. E. Nauer, H. Neugebauer and J. Theiner, *J. Electroanal. Chem.*, 1997, **420**, 301–306.
29 A. Giumanini, G. Verardo, E. Zangrando and L. Lassiani, *J. Prakt. Chem.*, 1987, **329**, 1087–1103.
30 P. Webb and C. Orr, *Analytical Methods in Fine Particle Technology*, Micromeritics, Norcross, GA, 1997.
31 K. Kaneko and C. Ishii, *Colloids Surf.*, 1992, **67**, 203–212.
32 H. Lee and W. I. Choi, *Phys. Rev. Lett.*, 2006, **97**, 056104.
33 J. Germain, F. Svec and J. M. J. Frechet, *Polym. Prepr. (Am. Chem. Soc., Div. Polym. Chem.)*, 2007, **97**, 272–273.

34 C. Buda and B. D. Dunietz, *J. Phys. Chem. B*, 2006, **110**, 10479–10484.
35 J. L. C. Rowsell, J. Eckert and O. M. Yaghi, *J. Am. Chem. Soc.*, 2005, **127**, 14904–14910.
36 R. C. Lochan and M. Head-Gordon, *Phys. Chem. Chem. Phys.*, 2006, **8**, 1357–1370.
37 M. Dinca, A. Dailly, Y. Liu, C. M. Brown, D. A. Neumann and J. R. Long, *J. Am. Chem. Soc.*, 2006, **128**, 16876–16883.
38 S. K. Bhatia, *Langmuir*, 2006, **22**, 1688–1700.
39 S. S. Kaye and J. R. Long, *J. Am. Chem. Soc.*, 2005, **127**, 6506–6507.
40 M. Dinca and J. R. Long, *J. Am. Chem. Soc.*, 2005, **127**, 9376–9377.
41 M. Dinca, W. S. Han, Y. Liu, A. Dailly, C. M. Brown and J. R. Long, *Angew. Chem., Int. Ed.*, 2007, **46**, 1419–1422.
42 A. Anson, J. Jagiello, J. B. Parra, M. L. Sanjuan, A. M. Benito, W. K. Maser and M. T. Martinez, *J. Phys. Chem. B*, 2004, **108**, 15820–15826.
43 P. M. Budd, A. Butler, J. Selbie, K. Mahmood, N. B. McKeown, B. Ghanem, K. Msayib, D. Book and A. Walton, *Phys. Chem. Chem. Phys.*, 2007, **9**, 1802–1808.
44 N. B. McKeown, P. M. Budd and D. Book, *Macromol. Rapid Commun.*, 2007, **28**, 995–1002.
45 B. S. Ghanem, K. J. Msayib, N. B. McKeown, K. D. M. Harris, Z. Pan, P. M. Budd, A. Butler, J. Selbie, D. Book and A. Walton, *Chem. Commun.*, 2007, 67–69.
46 N. B. McKeown, B. Gahnem, K. J. Msayib, P. M. Budd, C. E. Tattershall, K. Mahmood, S. Tan, D. Book, H. W. Langmi and A. Walton, *Angew. Chem., Int. Ed.*, 2006, **45**, 1804–1807.
47 A. B. Pangborn, M. A. Giardello, R. H. Grubbs, R. K. Rosen and F. J. Timmers, *Organometallics*, 1996, **15**, 1518–1520.
48 P. Tarazona, U. M. Marconi and R. Evans, *Mol. Phys.*, 1987, **60**, 573–595.
49 P. Tarazona, *Phys. Rev. A*, 1985, **31**, 2672–2679.
50 D. K. Moon, M. Ezuka, T. Maruyama and K. Osakada, *Makromol. Chem.*, 1993, **194**, 3149–3155.
51 H. Tamai, M. Hakoda, T. Shiono and H. Yasuda, *J. Mater. Sci.*, 2007, **42**, 1293–1298.
52 J. Stejskal, M. Trchova, S. Fedorova and I. Sapurina, *Langmuir*, 2003, **19**, 3013–3018.
53 D. H. Zhang and Y. Y. Wang, *Mater. Sci. Eng., B*, 2006, **134**, 9–19.